Chapter XX: Laser scanning of a complex cave system during multiple campaigns: a case study of the Domica Cave, Slovakia

Ján Kaňuk[1], Jozef Šupinský[1], John Meneely[2], Zdenko Hochmuth[1], Ján Šašak[1], Michal Gallay[1], Marco Callieri[3]

1 - Institute of Geography, Faculty of Science, Pavol Jozef Šafárik University in Košice, Jesenná 5, 04001 Košice, Slovakia

2 - School of Natural and Built Environment, Queen's University Belfast, Elmwood Avenue BT7 1NN Belfast, Northern Ireland, UK

3 - Visual Computing Lab, Institute of Information Science and Technologies, National Research Council of Italy, Pisa, Italy

1. Introduction

Caves are natural subsurface hollow forms with an extremely complex three-dimensional (3D) morphology in both horizontal and vertical directions. The caves have attracted people's attention since ancient times. Prehistoric man sought refuge from adverse weather and cold, but also wild animals or the enemy. Nowadays, the inherent mystery and natural beauty captivate human curiosity, therefore, the caves became the subject of tourism but also protection. From a scientific point of view, the caves are an important source of information about the past environment important for understanding contemporary conditions and changes. The history of nature can be reconstructed from the preserved natural materials, such as sediments, ice, geomorphological forms, tectonics, but also objects of organic or human origin like fossils, bones, working tools, paintings, ash, etc. The research of caves provides valuable knowledge for geology, hydrology, geomorphology, biology, cryosphere, but also history.

From the mapping perspective, the caves are a major challenge for the complexity of surface shapes, darkness, the presence of water, mud, or even ice, confined spaces (Gallay et al., 2015). At present, cave surveying is mostly performed by volunteer cavers, grouped in caving clubs and associations, to a lesser extent professional cavers conduct mapping and research of caves. Traditionally, mine surveying methods, such as tacheometry, have been used to locate the cave corridors and produce maps. Despite the immense effort of cave surveyors, the resulting maps contain highly generalized floor plans or projected vertical side views.

Currently, mapping with a laser distance measurer, inclinometer, and compass is widely used. Show caves or other spacious caves are mapped with a total station. The main part of the map comprises of traverse to which other measurements are connected. Typically, the position of side corridors, passages, large speleothems, water streams, lakes, or abysses is recorded. In this way, even today, most of the cave maps are created. The purpose is mostly focused on technical documentation of underground space showing the course of the cave, not any details or small-scale features. Other technologies based on underground global navigation system (U-GPS) (Wenger, 2004), sonar (Stipanov et al., 2008), ground-penetrating radar (Chamberlain et al., 2000), seismic (Beres et al. 2001), or electric resistivity methods

(Petersen and Berg, 2001) have been tested in the past to refine the mapping of caves. However, these methods still are not extensively applied in caves mainly for their complexity and demands on technical equipment and data processing. Over last the two decades, remote sensing technologies, such as close-range photogrammetry (Triantafyllou et al., 2019) and laser scanning (Mohammed Oludare and Pradhan, 2016), or their combined use (Lerma et al., 2010) gradually became popular in cave mapping. The methods are capable of capturing an unprecedented level of detail much faster than other methods used to date. Both methods generate millions of 3D point measurements (point cloud) representing the mapped surface highly accurately in the order of millimeters and without the need to generate a surveying traverse. The application of close-range photogrammetry is limited by suitable light conditions usually achieve by powerful artificial lights. In the case of laser scanning which uses light detection and ranging technology (i.e., lidar), the darkness of caves is not a problem. For this reason, lidar from terrestrial platforms has been increasingly used in mapping caves despite the technology is more expensive compared to digital cameras and lights needed for photogrammetry.

A distinction is made between terrestrial laser scanning (TLS) and mobile laser scanning (MLS). TLS is performed from static ground-based platforms (e.g. tripod, steel plate) by a laser scanner rotating around its axis while sending out laser light. It records the horizontal and vertical angle of the emitted laser beam and time until the emitted portion of the energy is returned as the echo. The scanner has to be placed in another location to capture the entire scene without data shadows during mapping. The individual point cloud originating from each scanning position of the scanner needs to be mutually oriented in the procedure of registration to generate a single point cloud in a common coordinate system. For the registration to be highly accurate and successful, a sufficient portion of the scans must overlap in space thus cover the same area although from different angles. The registration of individual scans is performed in dedicated software in the post-processing stage either manually or automatically. In recent years, a significant trend in TLS is the online processing of raw data, which involves automated self-registration of scans already during data collection.

The principle of MLS is based on the recordings of two synchronized devices: the inertial measurement unit (IMU) and the laser scanner. The IMU records the orientation angles along the x, y, z axes in 3D space to determine the trajectory of the laser scanner. The coordinates of the individual points recorded by the laser scanner are then calculated based on the laser triangulation (pulse emission angle and distance) with respect to the position of the scanner. The main benefit of MLS is in the speed of mapping and reduced data shadows by moving of scanner in space providing an opportunity to scan around any object. On the other hand, the limited ability to record the trajectory of the scanner's motion using the IMU compromises the accuracy of the 3D coordinates of the resulting point cloud. IMU locates itself by employing various sensors, such as gyroscope, accelerometer, compass, barometer, and GNSS. The basic problem is that the frequency of recordings by IMU is over 1000 times lower compared to the frequency of laser scanning. These shortcomings in tracking the scanner motion must be compensated by calculations, for example, using the simultaneous location and mapping (SLAM) method. This method is becoming widely used in MLS.

TLS is often preferred before MLS, for its higher positional accuracy and high spatial density of recorded points, in mapping complex cave morphologies (Oludare and Pradhan, 2016). Although there is a wide range of less costly surveying methods, lidar has a great potential to replace traditional techniques for cave mapping in the close future. We demonstrate the capabilities of TLS in this chapter by showing the results of mapping over 5000 meters of the Domica cave in Slovakia by TLS in various environmental conditions.

2. Review of the published works on laser scanning in caves

The application of laser scanning in caves dates back to the late 1980s when TLS focused on renowned sites such as Altamira between 1988 and 2001 (Donelan, 2002) or Cosquer Cave in 1994 (Thibault, 2001) which were mapped by active triangulation. However, the relatively short scanning range of triangulation scanners hampered their extensive application for being time-consuming and laborious. Today, this TLS approach is mainly used for detailed 3D scanning of smaller objects, using commercially available devices such as Kinect (Hämmerle net al., 2014), Faro Freestyle or iPhone 12 Pro.

Even after more than 30 years since the first TLS in caves, few cave systems were mapped in a large scale. We assume it is mainly related to caution when using a laser scanner in a cave, as the cost of such a device is still high (from 20,000 EUR to 150,000 EUR). An overview of works focused on mapping caves using TLS was presented in Gallay et al. (2015) or Oludare and Pradhan (2016). A large number of cave laser scanning projects remain unpublished or published in local magazines difficult to find.

Table 1 presents a chronological overview of publications demonstrating the use of TLS in various caves, the purpose of the mapping, the length of the mapped parts, and the scanners used. The list is not a complete overview, but it summarizes TLS projects providing details on the purpose for mapping, the technology used, or the recorded length of cave corridors. The simple analysis of the number of scientific papers in the Scopus database by using the query (TITLE-ABS-KEY (lidar AND cave)) OR (TITLE-ABS-KEY (laser AND scanning AND cave)) found 282 documents published since 1995. It indicates growth in laser scanning of caves which intensified since 2008 from about 5 up to 30 works published per year in 2020.

The review in Table 1 suggests that before 2010, laser scanning of caves was performed mainly for archaeological research in small but significant sites where a small number of scan positions was sufficient (up to 10) (Robson-Brown et al., 2001; Westerman et al., 2003; Gonzalez-Aguilera et al., 2009). Since 2010, laser scanning has been applied on a larger scale. The variety of scanners on the market and improved capabilities, lower price, and new methods of processing point clouds stimulated the application also in caves. Gradually, longer parts of caves were mapped, larger areas of caves with a larger number of scanning positions were performed. The main purpose was in cave documentation (Petters et al., 2011; Kuda et al., 2014; Zlot and Bosse, 2014; Kregar et al., 2019) and geomorphological analysis (Roncat et al., 2011, Buchroithner et al., 2012, Bella et al., 2015, Fabbri et al., 2017, Gallay et al. 2016). Other applications include, for example, analysis of cryomorphological characteristics of cave ice (Gašinec et al., 2012; Gómez-Lende and Sánchez-Fernández, 2018), as well as evaluation of the volume change of glacial glaze (Milius and Petters, 2012; Šupinský et al., 2019). TLS in caves was also used in zoology for animal counting purposes, in assessing potential natural risks, and in paleontology (Azmy et al., 2012; Lyons-Baral, 2012; Citton et al., 2017).

There are two main types of TLS technology. The most widely used scanners are based on emitting pulses of laser energy (time-of-flight scanners) which reach a longer range than the second type based on continuous emission of laser energy (continuous wave (CW), phase-based scanners). In narrow passages, however, the advantage of pulse-based laser scanners cannot be fully exploited. The deployed devices comprise pulse-based scanners Riegl LMS / VZ Series (Núñez et al., 2013; Tyszkowski et al., 2016; Šupinský et al., 2019), Leica ScanStation (Pukanska et al., 2017; Gómez-Lende a Sánchez-Fernández, 2018; Zeid et al., 2019), Leica BLK Series (Kregar et al., 2019); or phase-based scanners Faro Focus 3D X / S Series (Gallay et al., 2015; Aiello et al., 2019; Radicioni et al., 2019), Leica HDS Series (Marisco et al., 2015; Santagata et al., 2015; Nocerino et al., 2019), Z+F IMAGER (Roncat et al., 2011; Plan et al., 2013; Cosso et al., 2014). The list of reviewed works supports that TLS in caves is possible even in challenging conditions (Buchroithner and Gaisecker, 2009). In addition, MLS brings new possibilities for cave mapping (Bosse et al., 2012; Zlot and Bosse, 2014; Kaul et al., 2016).

Tab. 1. Summary of published works concerning laser scanning in caves.

Year	Author	Location	Country	Purpose of laser scanning mission	Range	Type of scanner device
1999	Perperidoy et al. 2010	Chapel's cave	USA	Documentation	Unknown	Unknown
2001	Thibault	Cosquer Cave (1994)	France	Archeology	Unknown	SOISIC
2001	Robson-Brown et al.	Dordogne Caves	France	Archeology	2 scans (wall)	Surveyor ALS
2002	Donelan	Altamira Cave	Spain	Archeology	Unknown	Minolta VI-700
2003	Caprioli et al.	Castellane Grotte Cave	Italy	Archeology	100 m	Mensi-GS100
2003	Westerman et al.	Peak Cavern Vestibule	UK	Archeology	Unknown	Riegl LMS-Z360
	El-Hakim et al.	Baiame Cave	Australia	Archeology	Unknown	Riegl LMS-Z210i
2004	The Courier (Channel 4 Time team)	Wemyss caves	Scotland	Archeology	Unknown	Unknown
2005	Aujoulat	Veilmouly Cave (1994)	France	Archeology	Unknown	SOISIC
2005	Fryer et al.	Baiame Cave	Australia	Archeology	Unknown	Riegl LMS-Z210i
2005	Murphy et al.	Gaping Gill Cave	United Kingdom	Documentation	Unknown	Riegl LMS-Z210i
2006	Beraldin	Grotta dei Cervi	Italy	Archeology	Unknown	Big Scan prototype
2006	Doering	Preacher's Cave	Bahamas	Archeology	20 m	Leica HDS 3000
2007	Tsakiri et al.	Kefala Cave	Greece	Documentation	Unknown	iQsun 880HE80
2008	Brich et al.	High Pesture Cave	United Kingdom	Documentation	Unknown	Trimble GS200
2008	Canavese et al.	Naica Cave	Mexico	Geology	110 m	FARO CAM2 Focus 3D
2009	Buchroithner & Geiseckner	Dachstein Southface Cave	Austria	Documentation	100 m	Riegl LMS-Z420i
2009	Gonzalez-Aguilera et al.	Las Caldas, Pena de Candamo Caves	Spain	Archeology	Unknown	Trimble GS200
2009	Chandelier & Roche	Tautavel Cave	France	Paleontology	Unknown	Trimble GS200
2009	Pucci & Marambio	Olerdola Cave	Spain	Archeology	Unknown	Riegl LMS-Z420
2009	Rüther et al.	Wonderwerk Cave	South Africa	Archeology	Unknown	Leica HDS3000
2010	Grussenmeyer et al.	Les Fraux Cave	France	Archeology	Unknown	FARO Photon 120
2010	Lerma et al.	La Cova del Parpallo Cave	Spain	Archeology	Unknown	FARO LS 880HE
2010	McIntire	Mushpot Cave	USA	Documentation	150 m	Leica HDS6000
2011	Addison	Mammoth Cave	USA		4 000 m	
2011	Buchroithner	Eisriesenwelt Cave	Austria	Cryomorphology	1 000 m	FARO Photon 120/20 (2011); FARO FOCUS 3D (2013)
2011	Canavese et al.	Santa Barbara Cave System	Italy	Geomorphology	740 m	Leica HDS6100 and Riegl LMS-Z210i
2011	Jaillet et al.	Orgnac's cave	France	Documentation	Unknown	Leica HDS 6000
2011	Petters et al.	Eisriesenwelt Cave	Austria	Cryomorphology	1 000 m	FARO Photon 120
2011	Roncat et al.	Marchenhohle Cave	Austria	Morphogenetic	150 m	Z+F Imager 5006i
2012	Azmy et al.	Gua Kelawar Cave	Malaysia	Zoology	14 scans	FARO Photon 120
2012	Buchroithner	Niah Caves	Malaysia	Documentation	Unknown	FARO FOCUS 3D
2012	Gašinec	Dobšinská Ice Cave	Slovakia	Cryomorphology	Unknown	Leica ScanStation C10
2012	Kordić et al.	Kuca Cave	Croatia	Archeology	Unknown	FARO Photon 120
2012	Lyons-Baral	Coronado Cave	USA	Hazards evaluation	200 m	Leica ScanStation C10
2012	Milius & Petters	Eisriesenwelt Cave	Austria	Cryomorphology	1 000 m	FARO Photon 120
2012	Santos Delgado et al.	El Sidrón Cave	Spain	Paleontology	50 m	Leica ScanStation C10
2013	Canevese and Tedeschi	Re Tiberio Cave	Italy	Documentation	60 m	Leica HDS6100

2013	Gede et al.	Pálvölgy Cave	Hungary	Documentation	Unknown	FARO Focus 3D, Leica ScanStation C10
2013	Lindgren & Galeazzi	Las Cuevas Cave	Belize	Documentation	Unknown	FARO Focus 3D
2013	McFarlane et al.	Gomatong Caves	Malaysia	Documentation	1 000 m	FARO Focus 3D
2013	Nash & Beardsley	Cathole Cave	Wales	Documentation	Unknown	Leica HDS6000
2013	Núñez et al.	Can Sadurní Cave	Spain	Archeology	Unknown	Riegl LMS-Z420i
2013	Plan et al.	Mammuthöhle Cave	Austria	Geomorphology	200 m	Z+F Imager 5006i
2013	Puchol et al.	Pastora Cave	Spain	Archeology	Unknown	FARO Photon 120
2013	Silvestre et al.	Algar do Penico Cave	Portugal	Documentation	80 m	Leica ScanStation C10
2013	Yumin	Lianhua Cave, Tianlongshan Cave	China	Archeology	Unknown	Unknown
2014	Berenguer-Sempere et al.	Castil Ice Cave	Spain	Cryomorphology	72 m	Leica ScanStation C10
2014	Burens et al.	Les Fraux Cave	France	Archeology	430 m	FARO Photon 120, FARO Focus 3D
2014	Cosso et al.	Arma Pollera Cave	Italy	Documentation	Unknown	Z+F Imager 5010
2014	Hämmerle et al.	Dechen Cave	Germany	Comparsion	Unknown	Riegl VZ-400, Kinect
2014	Hobléa et al.	Orgnac's Cave, Chauvet Cave	France	Documentation	Unknown	Leica HDS 6000
2014	Hoffmeister	Sodmein Cave	Egypt	Archeology	Unknown	Riegl LMS-Z420i
2014	Kukutsch et al.	Amatérska Cave	Czechia	Documentation	1 300 m	Leica ScanStation C10
2014	Leonov et al.	Denisova Cave	Russia	Documentation	37 scans	FARO Focus 3D
2014	Novaković	Škocjan Caves	Slovenia	Documentation	Unknown	Leica ScanStation C10
2014	Tyree	Skoteino Cave	Greece	Documentation	Unknown	Riegl LMS-Z420i
2014	Zlot & Bosse	Jenolan Caves	Australia	Documentation	17 100 m	Hannibal, Zebedee
2015	Bella et al.	Dupnica Cave	Slovakia	Geology	Unknown	Leica ScanStation C10
2015	Gallay et al.	Domica Cave	Slovakia	Geomorphology	1 600 m	FARO Focus 3D
2015	Marisco et al.	Santa Croce Cave	Italy	Documentation	90 m	Leica HDS 3000
2015	McFarlane et al.	Gomantong Caves	Malaysia	Zoology	1 000 m	FARO Focus 3D
2015	Santagata et al.	Grotta della lucerna Cave	Italy	Documentation	Unknown	Leica HDS 7000
2016	Hoffmeister	Ardelas Cave	Spain	Documentation	Unknown	Riegl LMS-Z420i
2016	Kruger et al.	Rising Star Cave	South Africa	Archeology	Unknown	FARO Focus 3D
2016	Tyszkowski et al.	20 Caves	Poland	Documentation	Unknown	Riegl VZ-400
2016	Yakar et al.	„Hadim“ Cave	Turkey	Documentation	13 scans	OPTECH ILRIS
2017	Basantes et al.	Elviandi Cave	Ecuador	Documentation	450 m	FARO Focus 3D
2017	Citton et al.	Grotta della Básura Cave	Italy	Paleonthology	Unknown	Leica ScanStation 2
2017	Fabbri et al.	Grotta A Cave	Italy	Geology	Unknown	FARO CAM2 Focus 3D
2017	Pukanska et al.	Belianska Cave	Slovakia	Documentation	Unknown	Leica ScanStation C10

2018	De Waele et al.	Ca'Castellina Cave	Italy	Geomorphology	Unknown	FARO CAM2 Focus 3D
2018	Gómez-Lende & Sánchez-Fernández	Picos de Europa Ice Caves	Spain	Cryomorphology	Unknown	Leica ScanStation C10, FARO Focus 3D
2018	Petrović et al.	Pećura and Zamna Caves	Serbia	Documentation	Unknown	Leica Nova MS50
2019	Aiello et al.	Grotta dei Pipistrelli	Italy	Documentation	72 scans	FARO Focus S70
2019	Kregar et al.	Kumik Cave	Slovenia	Documentation	2 000 m	Leica BLK360
2019	Nocerino et al.	Grotta Giusti	Italy	Documentation	Unknown	Leica HDS7000
2019	Radicioni et al.	Frasassi Caves	Italy	Documentation	Unknown	FARO Focus 3D
2019	Shults et al.	Kyiv Pechersk Lavra caves	Ukraine	Documentation	Unknown	Leica ScanStation
2019	Sorrioux et al.	Gouffre Georges	France	Geology	250 m	Riegl VZ-1000
2019	Šupinský et al.	Silická ľadnica Cave	Slovakia	Cryomorphology	50 m	Riegl VZ-1000
2019	Šupinský et al.	Domica Cave	Slovakia	Documentation	6 000 m	FARO Focus 3D, Riegl VZ-1000
2019	Zeid et al.	Fumane Cave	Italy	Archeology	Unknown	Leica ScanStation C10

3. Laser scanning of the Domica Cave

The presented case study concerns laser scanning of the Domica Cave and its exterior surroundings. The resulting geodatabase allows for creating highly-detailed and highly accurate maps and side views of the cave but also means for geomorphological, climatological, speleobiological, and hydrological research of the cave. TLS has been carried out gradually since 2014. First, the show cave part was scanned (ca. 1,500 m), and then the other publicly unavailable parts followed. In 2014, an airborne laser scanning (ALS) campaign was carried out to map a wider area.

3.1 Geographical setting

Domica originated in the Triassic limestones of the Slovak Karst Mountains in south-eastern Slovakia, about 1 km west of the border with Hungary (Fig. 1). The cave is a beginning part of a much longer system continuing through the state border into the Aggtelek Karst where it is called Baradla Cave. The Domica-Baradla cave system has a total length of 27,476 m (Gaál and Gruber, 2014). The part in Slovakia (Domica) has a length of 8,014 m. It is a unique cave with colorful flowstone decoration, which is characterized mainly by cascading lakes, typical onion-shaped stalactites, flowstone drums, and shields, as well as stegamites. The uniqueness of the cave is also emphasized by specific fauna and flora. For these reasons, the cave is a listed UNESCO World Natural Heritage Site and a Ramsar site. The detailed characteristics of the entire Domica-Baradla cave system are in Gaál and Gruber (2014).

The cave has been formed by underground streams, two of which still flow through: the Domický stream and the Styx river, which further continues to the Hungarian part. Domica Cave is regularly affected by floods mainly induced by rain-on-frozen-soil in winter. The floods have a destructive effect on the decoration of the cave, as well as on the infrastructure in the accessible part of the cave. The presence of tourist visitors also induced anthropogenic interventions in the cave such as building water dam pavements. A better understanding of the reoccurring floods were one of the rationales behind the application of TLS and ALS to achieve a detailed representation of the cave.

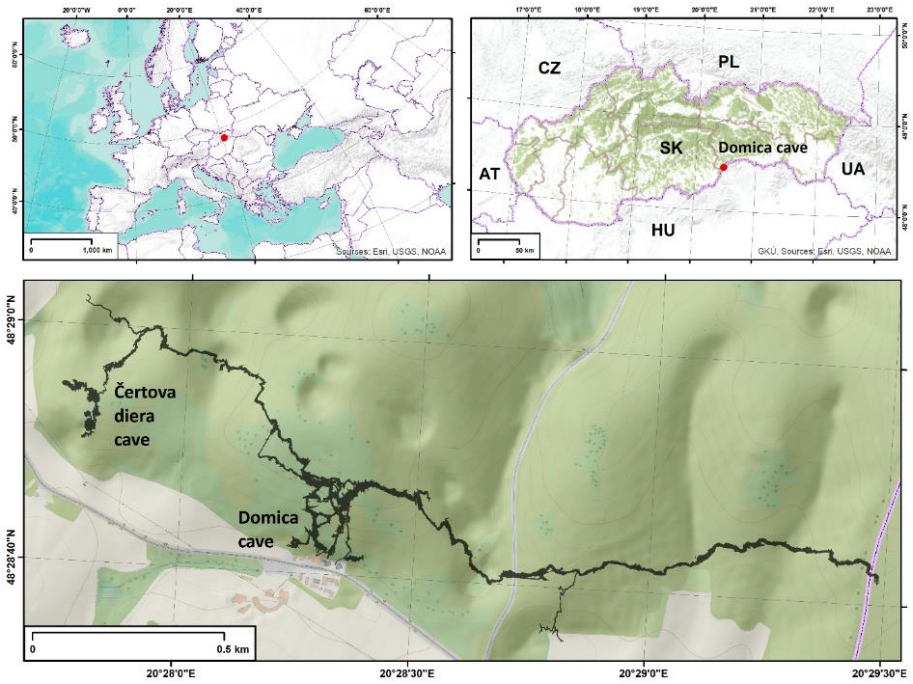

Fig. 1. Location of the Domica cave system including the Devil's hole cave (Čertova diera) overlayed with shaded airborne lidar digital terrain model and land cover map © Open Street Map.

Domica Cave was mapped several times since its discovery in 1932 by a soldier Ján Majko. Traditionally mine surveying methods and equipment were used for mapping. Just after the discovery, the first comprehensive mapping of Domica was supervised by mining surveyor Paloncy. The aim was to generate a map of the new cave in the territory of former Czechoslovakia. At that time, the cave comprised prehistoric artifacts untouched since the neolithic people left the cave probably because of the fall of entrance over 5,000 years ago. In 1937, Roth carried out a much more detailed mapping, which focused on large halls rich in cave decoration. He produced a very detailed map of selected parts of the cave at a scale of 1: 100. The purpose of surveying the cave in 1949 was in locating and establishing the underground state border with Hungary. The mission resulted in a highly accurate and well-stabilized surveying network with detailed documentation of the measurements. In 1964, a map created by Dropp and Chovan was published, complementing the cave floor plan with side views. Further mapping by Droppa (1972) recorded the levels of cave passages indicating a gradual change of erosion base during the cave formation (Droppa, 1972). The successive opening of new parts of the cave led to greater invasive interventions in the interior of the cave. In order to build an artificial tunnel from Suchá chodba to Panenská chodba passages, a detailed mine surveying was carried out in 1975 (Novoveský, 1975). The stabilized surveying points are still present and can be used for connecting new measurements with high accuracy. Hochmuth (2014) linked to the existing points from the previous mapping campaigns using traditional mine surveying techniques. The aim was to make a continuous traverse through the cave and map also the parts that have not been measured before.

3.2 Laser scanners used in mapping the cave

There were two types of scanners used for TLS in Domica. First, the phase-based FARO Focus 3D X 130 laser scanner was deployed. The advantage was in its small size and weight (about 5 kg) which made it easily portable and easy to handle in the narrow passages of the cave. The device scans at ranges between 0.6 - 130 m providing distance measurement at ± 2 mm of precision using near-infrared laser energy of 1,550 nm wavelength. Its benefit is in a wide vertical field of view of 310 °, which allows for scanning ceilings above the scanner. We used measuring spheres of uniform diameter as targets for the semiautomated registration of scans but it is not necessary now for the advances in adjustment software routines.

Since 2015, we commenced scanning with a RIEGL VZ-1000 scanner which is primarily developed for outdoor long-range surveying. Nevertheless, its use in cave mapping is common (Table 1). It is a full waveform pulse-based scanner emitting near-infrared laser pulses of 1,550 nm wavelength. The measurement precision along the range direction is ± 3 mm with a minimal scanning range from 1.5 m to 1,400 m. Compared to the FARO scanner, the VZ-1000 is relatively heavy (10 kg with batteries), which makes it difficult to handle in the cave. The most significant drawback of the scanner in caves is the limited vertical scanning angle up to 100 ° which complicates capturing data on the ceiling right above the scanner. The data shadows created in this way have to be eliminated by the closer placement of scanning positions to each other or by vertical scanning of the ceiling if the scanner is tilted.

Besides the distance between consecutive scanning positions, the density of point measurements is controlled by the frequency of measurements. The RIEGL VZ-1000 is capable of emitting 550,000 pulses per second (550 kHz pulse repetition rate). Scanning at this frequency takes approximately 1 minute and 20 seconds with a scanning detail of 0.06 ° in the vertical and horizontal directions. The measurement frequency of the FARO Focus 3D X 130 is up to 950,000 points per second and at resolution ¼ (0.036 °), scanning from one position takes approximately 3 minutes and 26 seconds. The VZ-1000 is capable of recording an unlimited number of pulse echoes. Practically, only echoes above a set quality threshold are recorded and they can be further filtered based on pulse waveform deviation or rescaled intensity. This information can be used to remove stray points. From our experience, the data acquired with the VZ-1000 scanner contained fewer noise points than the data from scanning with FARO Focus 3D.

3.3 The workflow of lidar cave mapping

The TLS data acquisition is followed by several steps of data processing. The first task is in mutual orientation (registration) of individual point clouds acquired from scanning positions. The first two steps in Figure 2 take most of the time from the whole TLS surveying mission. Scanning positions needed to be carefully chosen to keep their number reasonably low, but minimizing the data shadows, ensuring an overlap of the consecutive scans. Ultimately, a carefully planned TLS survey allows for the application of automated procedures for adjusting the scan positions and resulting in minimized registration errors, typically in the order of millimeters. Gallay et al. (2015) explain the details of the TLS methodology of scanning in 2014 and Šupinský et al. (2019) describe the following TLS campaigns. The main steps of the workflow to generate a cave map are shown in Figure 2.

After the scans are joined into a single point cloud, it is necessary to filter out the points which are for various reasons a result of an error (Kaňuk et al., 2019). These are mainly the points that form as laser reflections from the water, stray points, or points of high position uncertainty for low surface reflectivity. Point filtering and the denoising process is a prerequisite for deriving complex and realistic 3D cave surface models. However, the purpose of the final 3D model has to be always considered before its creation (Gallay et al., 2016). To create a cave map, the TLS has to focus on data acquisition of the bottom of the cave to respect the floor plan principle. Then it is possible to extract the points representing

the cave floor including important features of the cave, such as cave boundaries, watercourse bed, cave decoration, fault lines.

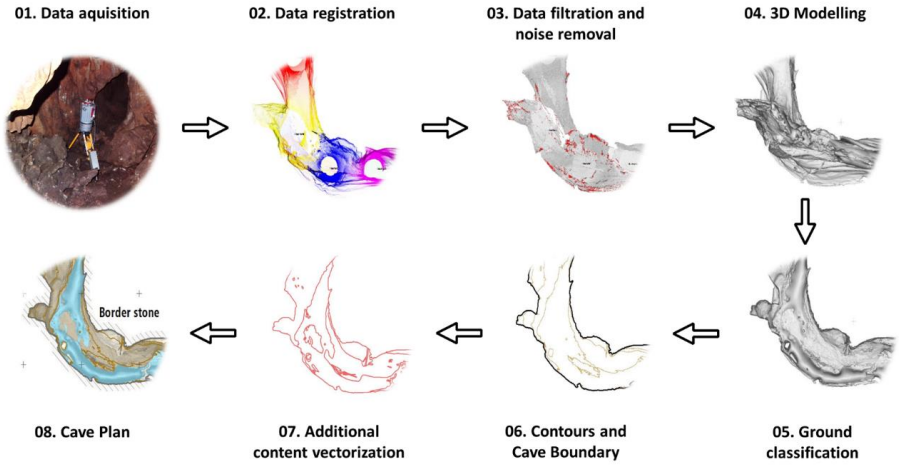

Fig. 2. The workflow of converting the TLS point cloud into cave map.

3.4 The multifold cave laser scanning campaign

Data collection was carried out in 43 campaigns summing to 178 scanning hours. From the practical point of view, the most time-consuming factor was in ensuring safe transport of the surveying equipment to the location of scanning and stabilization of the device in very narrow passages and areas with water and mud. To date, the mapping involved 1029 scan positions with the Riegl VZ-1000 scanner and 786 positions with the Faro Focus 3D scanner with an average of 9 million points per position. An average day involved 4-8 hours of scanning from about 46 positions. We placed the consecutive scan positions every 2 to 20 meters to ensure sufficient scan overlap. The achieved point density ranges between 26,000 points.m^{-2} in large domes to 460,00 points.m^{-2} in narrow passages.

The first phase of mapping was performed in March 2014 by John Meneely of Queen's University in Belfast with the FARO Focus 3D scanner (Gallay et al., 2015). The scanning involved 327 positions during the 5-day campaign focusing mainly on the show cave part with relatively comfortable access (Fig. 3C). The bottom of several narrow passages was covered by dry clay or limestone. Approximately 1,600 m of corridors and the exterior surroundings of the main cave entrance were mapped.

The following period 2014 to 2017 focused on data processing and 3D modelling of the cave surface (Gallay et al., 2016; Hofierka et al., 2017). Systematic extension of TLS into other parts of the cave started in 2017. First, we focused on scanning the parts with large domes and corridors. Thanks to the low water level of the underground Styx River, the riverbed could have been mapped along its entire length. We linked to the point cloud from 2014 by scanning the parts with artificial water dams which make boat trips possible in the cave. There was no water present but the bottom of the river bed was covered by mud. To avoid the sinking of the scanner in the mud, a platform was made from wooden boards which stabilized the scanner during data collection (Fig. 3D). In this way, parts of the cave up to the border with Hungary were mapped.

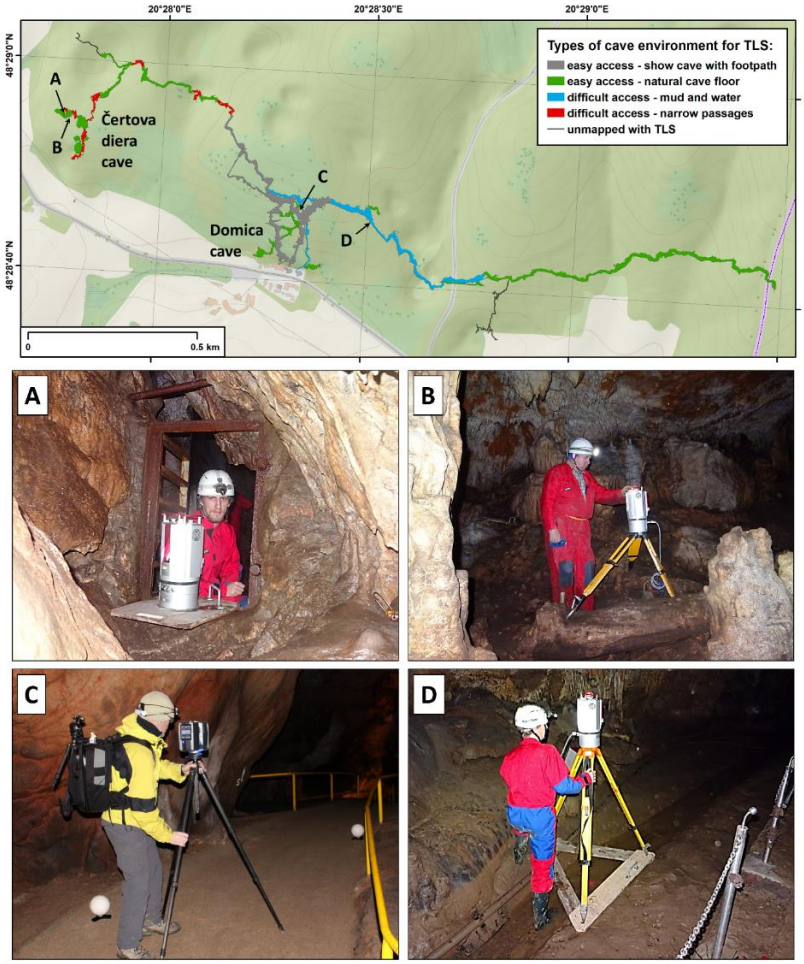

Fig. 3. Various kinds of environmental conditions while laser scanning the Domica cave are annotated with letters A-D and located on the map.

In 2018, the TLS mapping focused mainly on the Čertova diera Cave (Devil's Hole) where the cave system begins. This part of the cave is characterized by the altering of spacious domes and narrow passages where we had to crawl to pass through. the dimensions of the corridors did not allow the scanner to be placed on a tripod, therefore, to scan these parts, a steel platform was made on which the scanner is mounted with a screw (Fig. 3A). TLS in these parts of the cave was carried out only in the periods of low water level of the river Styx. In this way, a total of approximately 6,000 m of corridors were surveyed by TLS. The main challenge was in adopting the TLS to various types of material of the cave bottom such as concrete walkways, rock, mud, sand, and water. Consecutive scanning of the narrowed passages in Čerotva diera Cave required placing scan positions more closely to achieve overlaps of the acquired point clouds for their mutual orientation in the data post-processing stage. Another challenge was in processing the recorded big volume of data. The resulting point cloud contains over 25 billion points. For this reason, we optimized the individual scans and the captured level of detail.

A very important phase is cleaning and filtering of data to remove unnecessary points including data noise, blunders, or persons represents about 10% of the final point cloud (Hofierka et al. 2017).

The key procedure of the TLS data post-processing was in the mutual orientation of scans. This task was performed in the dedicated software of the scanners' vendors, FARO Scene and RIEGL RiScanPro, respectively. At least, four identical points between consecutive and overlapping scans need to be co-located. The white spheres (Fig. 3C) were used to achieve the registration in the first Domica TLS survey of 2014 (Gallay et al., 2015). The scans acquired in the following campaigns by RIEGL VZ-1000 were co-registered without any reflective artificial targets by, first, manually finding four identical points in the overlapping scans followed by an automatic coarse orientation. Then, an automatic Multi-Station Adjustment (MSA) procedure was used with the robust fitting mode to closely match the scans based on their area of overlap. This step resulted in finding groups of points, i.e. polydata, which represent identical parts of the scanned surface within the specified radii. By this means, the number of points used in the subsequent MSA procedure (registration) increased providing a more accurate registration of scanning positions (Ullrich et al. 2003). For the coarse registration, the standard deviation ranged from 8 to 15 mm, but and after the subsequent iterations of MSA, the resulting standard deviation of the internal registration of positions improved to 3 mm.

The integration of the first point cloud from 2014 with the subsequent point clouds was solved by importing all individual positions scanned in 2014 into the registration project in RiSCAN Pro and registering them with the rest of the scanned data. After the first stage of registration, the MSA procedure was used to closely match the scans which formed a closed traverse loop. The first position remained fixed and all other scan scenes were consequently aligned to each other in sections. When closing the scan survey loop of the 2014 data, the accumulated standard error was markedly reduced. For example, a 150 mm error accumulated at 150 positions. The error was compensated by a millimetre per position so that the resulting standard deviation of registration between scans decreased to 4 mm overall. The survey traverse could not be closed in the long passage from the Second water dam (east of Majkov Dome) to the Hungarian border.

To generate a continuing traverse from the underground state border with Hungary to the Majkov Dome, it was inevitable to cross the two water dams in the show cave part. This was possible for a low water level at the time of scanning enabling it to move through the bottom. Despite the favorable conditions, the sediment was unstable for placing the scanner securely on a tripod. Therefore a wooden platform was produced and used in such parts for stable positioning of the scanner (Fig. 3D). The platform was also used to boat the scanner on the water without turning the scanner off or repeatedly taking it apart. After scanning via the second water dam (2. plavba) the scanning continued above the ground through the second man-made exit from the cave where RTK-GNSS control points were measured. The registration error is the highest in the part from the second entrance to the Hungarian border as the scanning survey traverse remains unclosed (i.e. open). Therefore, the cumulated standard deviation of error could reach up to 200 mm. Such a large error could not have been much reduced even if artificial targets (e.g. spheres) are used unless the traverse is a closed loop. Moreover, the use of such targets was not feasible in such extreme environmental conditions in this part of the cave. Hence, manual identification of identical points and the iterative MSA procedure was preferred as the most appropriate solution.

After all the scans were mutually oriented, the resulting point cloud was georeferenced in the national coordinate system (EPSG code: 5514 S-JTSK Křovák East North). The procedure made use of 56 stabilised points located by precise mine surveying mapped by Novoveský (1975). The points were identified in the scans. We used conditions for finding correspondencies to at least 8 reference points and georeferencing errors of less than 50 mm. The resulting standard deviation of placing data do the national coordinate system is 0.016 m. The TLS cave data were complemented with an airborne lidar (ALS) point cloud supplied by the company Photomap. More details on the ALS data can be found in

Hofierka et al. (2017, 2018). The data supplier claims a 100 mm standard deviation of the georeferencing the ALS data based on control points measured with RTK-GNSS in open areas.

The effort in the cave resulted in the successful integration of TLS data acquired in multiple surveys using two types of scanners. Redundant points were removed from the point cloud based on filtering with the pulse-echo deviation above the value 20 and only the first and single returns were left. Such points resulted from scattered reflections on sharp edges on railings, speleothems, or stairs. Some kinds of unwanted points had to be removed manually. We observed mirrored features as point clusters in cases where the speleothems were covered with a thin water film. When scanning in winter near the cave exit, cold air mixed with the warmer air of the cave causing a lot of noise points at the floor and the cave ceiling. Therefore, in such environmental conditions, we recommend scanning when the air temperature gradient is low, ideally without wind in the exterior. After the point cloud was cleaned, its point density was unified by decimating the point cloud at the 10 mm level resulting in 2,000 million points. The extent of the final point cloud is shown in Fig.4.

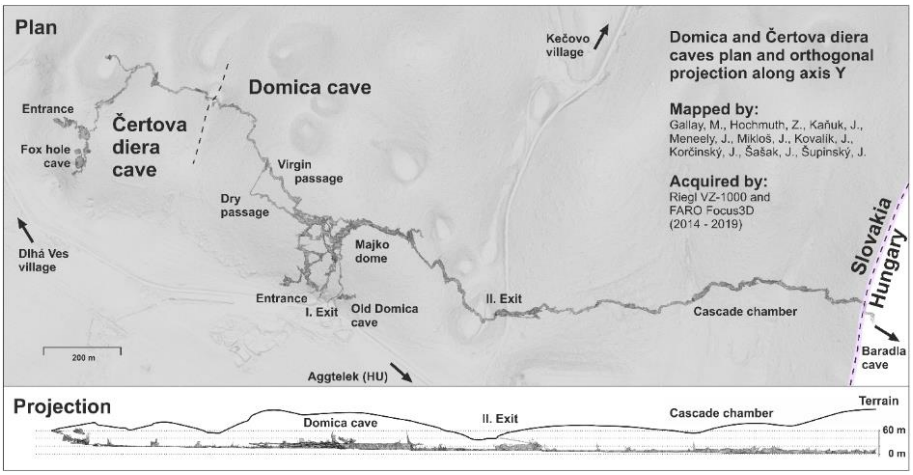

Fig. 4 Top view and side view of the Domica cave system resulting from multiple TLS campaigns combined with an airborne lidar digital terrain model.

3.5 Generating the 3D cave surface model

The point cloud of the cave allows for precise measurements, generating cross-sections and visualisation. However, volume calculations, advanced analyses of the cave surface such as geomorphometry or water flow modelling require the creation of a 3D digital surface model. The key prerequisite for this task is in the calculation of normal vectors for each to define the interior of the cave. Various approaches exist but for the complex cave surface morphology, the orientation of the normal is usually incorrectly determined if the normal point vectors are derived based on a simple neighborhood analysis, especially on speleothems and various isolated objects. For this reason, the normal vectors need to be oriented with respect to the scanner position for each scan. After this step, the normals are correctly defined and a correct surface model of the entire cave be derived.

The Screened Poisson surface reconstruction interpolation method (Kazhdan and Hoppe, 2013) implemented in the open-source software CloudCompare (Girardeau-Montaut, 2018) was used to derive the model in the form of a 3D mesh (Fig. 5). The quality of the resulting surface depends mainy on the presence of data voids, noise, and level of detail of the collected data and the spatial resolution of the output model. Other parameters such as Samples per node and point weight are significant in case

abundant noise points or local heterogeneity in point density exist in the input point cloud. For the full depth parameter, it fills in the areas with missing data using the defined spatial resolution. After creating the surface of the cave, it is necessary to cut out the area of interest for simulations. This step must be taken only after modeling the surface, because due to the interpolation function, deformations occur at the edges of the cropped area on the digital model, when the so-called "border effect" occurs.

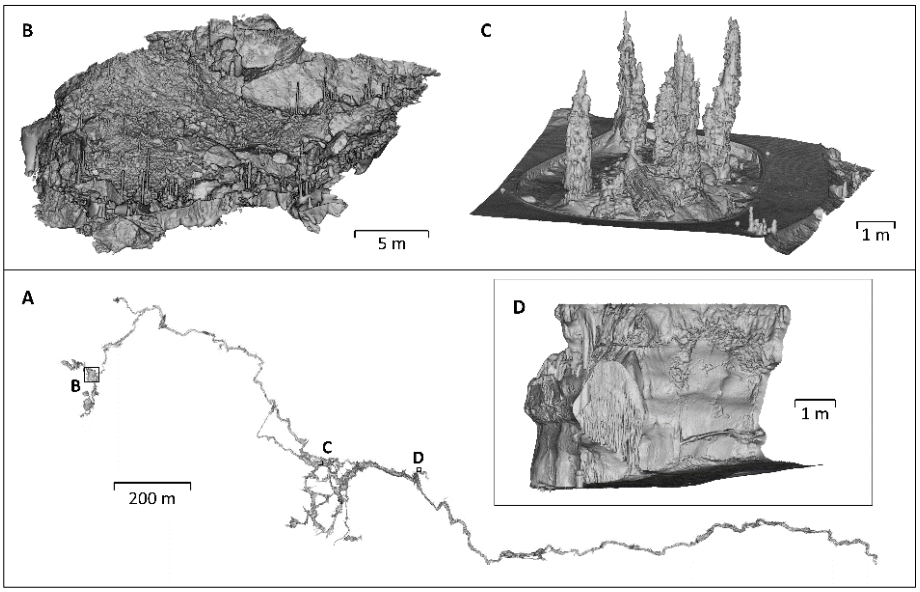

Fig. 5. Selected parts of the 3D cave surface model (A) showing the level of detail preserved in the model of thin ceiling stalatites (B), massive stalagmites of the Dome of the Indian Pagodas (C) and a stegamite (D).

3.6 New means of cave visualisation and application

The high level of detail and spatial extent of the scanned cave system opens new possibilities into how visualising the cave can be approached and communicated to other academics, professionals, or the general public. The traditional speleocartography can be enhanced by deriving the outlines of plnnar views from the 3D data and including the shaded surface model coloured by certain attributes, e.g. rock material or a morphometric parameter relief. The perception of the cave space becomes more accurate and information-rich (Fig. 6).

However, a map is still a static 2D means of visualising the 3D cave space. Recent developments in web-based 3D technologies have enabled interactive visualisation and analysis of large 3D point clouds which in turn enhances communication of the scientific results to a wider audience providing appealing means for research presentation, dissemination, and further analysis (Scopigno et al., 2017). It is now possible to integrate the 3D content on the Web directly into the browser without plug-ins or additional components. For example, Silvestre et al. (2015) presented an approach in which X3-D, WebGL, and X3-DOM were used to enable online 3D visualization and navigation of the interior of the Algar do Penico cave, Portugal, in several different Web browsers. Potenziani et al. (2015) introduced their 3-D Heritage On-line Presenter (3-DHOP), which is an open-source software package for the creation of interactive Web presentations of high-resolution 3-D models.

These reasons motivated us to generate a stand-alone LiDAR Web portal enabling other researchers, professionals or the public to explore the dataset without any need for special skills in computer graphics, geographic information science, installation of special software, or any additional plugins. Only a standard web browser and internet connection are required. The web portal was generated using the laspublish software utility of the LAStools package (Rapidlasso, 2019) which uses the Portree open-source WebGL based renderer (Scheiblauer 2014; Schuetz, 2016; Potree, 2021). Portree is capable of efficiently visualizing nearly 600 billion points in real-time via the Internet, changing colouring of points, performing measurement of 2D and 3D length, 3D area, volumes, generating vertical profiles, and exporting data. Fig. 7 demonstrates these capabilities and the presented dataset can be accessed via the link: https://uge-share.science.upjs.sk/webshared/Laspublish/Domica/Domica_Liscia.html

To display the 3D cave surface and its parameters, we generated a tool for interactive visualization online via the internet using the platform of the 3-DHOP (http://3-Dhop.net/). The tool showing the Domica cave as a 3D mesh is available at http://vcg.isti.cnr.it/varie/cave/ (Fig. 8). The interface enables zooming, rotation, panning, changing the source light direction, and measuring Euclidean 3-D distances between two points. The model was generated in Meshlab from a reduced number of input points (3.13 million) with the octree depth of 13. More details are presented in Gallay et al. (2016). Further use in 3-DHOP required conversion of the model into the compressed NEXUS format (http://www.vcg.isti.cnr.it/nexus/), which is based on a multi-resolution data structure (Cignoni et al., 2005). The format allows the client to efficiently perform view-dependent visualization for faster streaming and smooth rendering in the browser. The size of the model was reduced from 148 MB in the PLY format to 20 MB after conversion.

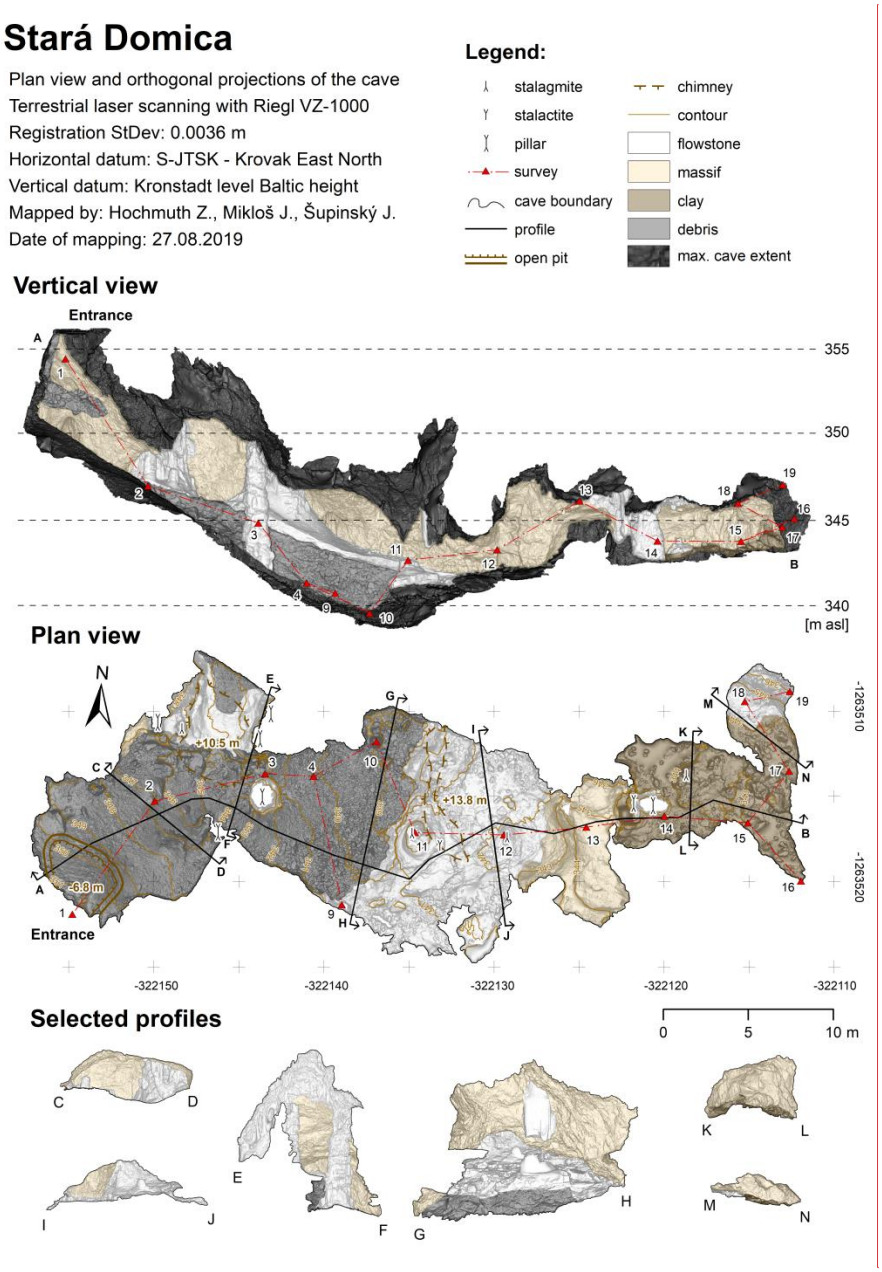

Fig. 6. Example of a cave map of a part of the Domica system called Stará Domica (Old Domica, Fig. 4) resulting from the TLS campiangs. The map contains shaded relief of the cave bottom DEM coloured according to the bottom material.

Commented [M1]: Tu navrhujem vymenit obrazok za celu jaskynu dno / Staru domicu – tento obrazok ide do Journal of maps

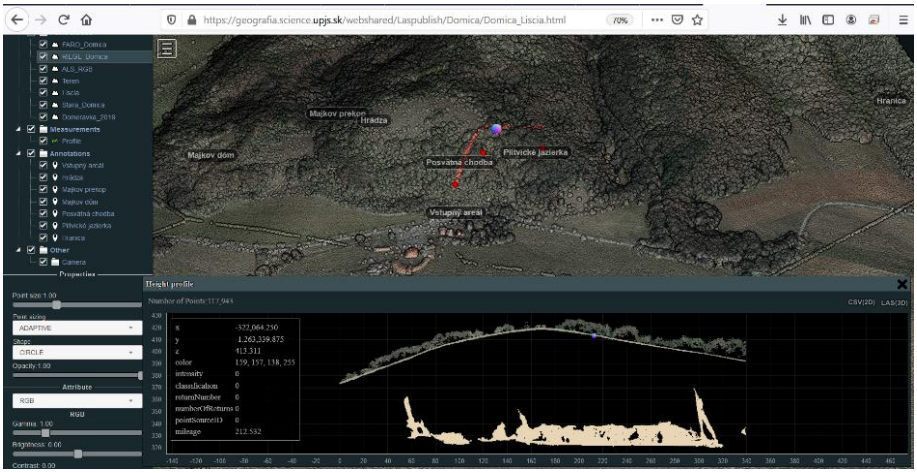

Fig. 7. Interactive online 3D visualisation and analysis of the cave 3D point cloud combined with airborne lidar via the Potree interface (Schütz et al. 2020). https://uge-share.science.upjs.sk/webshared/Laspublish/Domica/Domica_Liscia.html

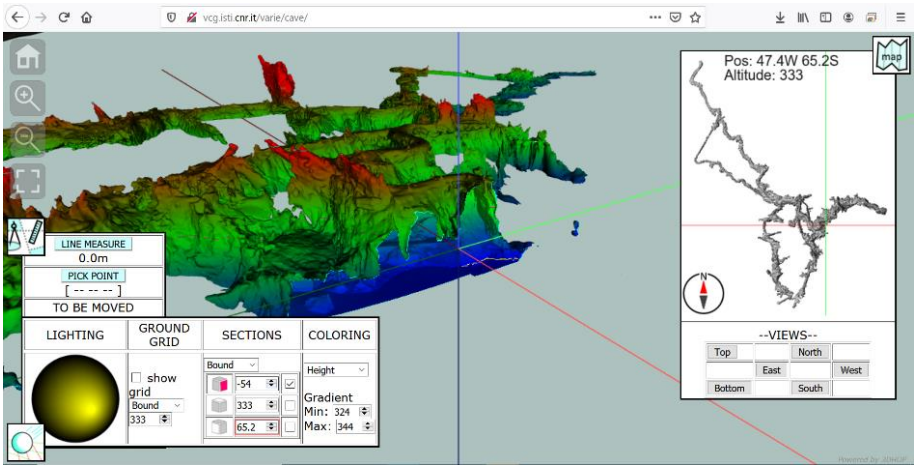

Fig. 8. Interactive online 3D visualisation and analysis of the cave surface model via the 3DHOP interface (Potenziani et al. 2015). http://vcg.isti.cnr.it/varie/cave/

The scientific and application potential of the TLS cave data is not only in more accurate measurement and maps but in other fields. Gallay et al. (2016) presented a study of ceiling channels in Domica by application of 3D morphometric parameters derived from the 3D mesh. These speleoforms are practically impossible to access in the height of 3 – 10 meters above the bottom. Therefore the 3D modelling allowed measuring cross-sections, extracting the channels, and providing evidence for

anastomosys of Styx as a significant process forming the cave system. Figure 9 presents an example of simulating a real flood event by the Delft3D FM (D-FlowFM, https://oss.deltares.nl/web/delft3d/home) modelling tool in which the accurate and highly detailed 3D model of the cave bottom is the main input. Such a modelling can be used to test the measures taken in the cave exterior and interior in several scenarios to find the most appropriate solution.

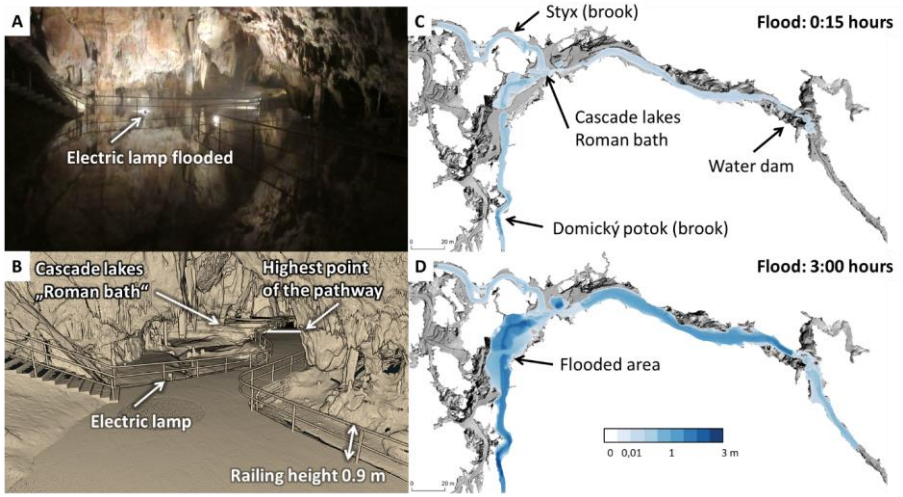

Fig. 9 Cave flood in Majkov Dome (10 February 2016) with a marked light source (A) and the point cloud of the dome (B). Water depth during the simulated flood event after 15 minutes (C) and 3 hours (D) of water inflow from the south-west and north-west (0.1 $m^3.s^{-1}$), outflow at water dam set to 0.14 $m^3.s^{-1}$.

4. Conclusions

TLS of Domica commenced in 2014 within a research project focused on developing new methods of 3D spatial modelling and surface analysis. The aim was the generating a 3D point representation of the cave with ultra-high spatial resolution so that cave surface morphology could be studied and linked with above-ground geomorphology. The research project resulted in findings of new speleofeatures, proving cave anastomosys by 3D geomorphometry or new means of 3D visualistion and modelling the floods reoccurring in the cave. The multifold TLS campaigns resulted in scanning over 5,000 m of corridors and experience in the scanning of various kinds of cave passages in diverse environmental circumstances. The acquired data contribute to more informative and more accurate cave maps, scientific research of features inaccessible from the human perspective, sustainable cave management, and new interactive visualizations easily accessible via the internet.

5. Acknowledgements

The presented research originated thanks to the financial support of the Ministry of Education, Science, Research and Sport of the Slovak Republic under the grant nr. VEGA 1/0300/19 and VEGA 1/0798/20.

6. References

Addison A., 2011 - LIDAR at Mammoth Cave. Civil Engineering Surveyor, April 2011: 22-25.

Aiello, D., Basso, A., Spena, M. T., D'Agostino, G., Montedoro, U., Galizia, M., ... & Santagati, C. (2019). The virtual batcave: A project for the safeguard of a UNESCO WHL fragile ecosystem. International Archives of the Photogrammetry, Remote Sensing & Spatial Information Sciences.

Azmy S.N., Sah S.A., Shafie N.J., Ariffin A., Majid Z., Ismail N.A. & Shamsir S., 2012 - Counting in the dark: Non-intrusive laser scanning for population counting and identifying roosting bats. Scientific Reports, 2: 524. http://dx.doi.org/10.1038/srep00524

Basantes, J., Godoy, L., Carvajal, T., Castro, R., Toulkeridis, T., Fuertes, W., … Addison, A. (2017). Capture and processing of geospatial data with laser scanner system for 3D modeling and virtual reality of Amazonian Caves. 2017 IEEE Second Ecuador Technical Chapters Meeting (ETCM). doi:10.1109/etcm.2017.8247455

Bella, P., Littva, J., Pukanská, K., Gašinec, J., Bartoš, K. (2015). Use of terrestrial laser scanning for the investigation of structural geological discontinuities and morphology of caves: on the example of the Dúpnica Cave, Západné Tatry Mts., Slovakia. Acta Geologica Slovaca, 7(2), 92-102.

Beraldin, J. A., Blais, F., Cournoyer, L., Picard, M., Gamache, D., Valzano, V., ... & Gorgoglione, M. (2006). Multi-resolution digital 3D imaging system applied to the recording of grotto sites: the case of the Grotta dei Cervi.

Berenguer Sempere F., Gómez-Lende M., Serrano E. & de Sanjosé-Blasco J.J., 2014 - Orthothermographies and 3D models as potential tools in ice cave studies: the Peña Castil Ice Cave (Picos de Europa, Northern Spain). International Journal of Speleology, 43 (1): 35-43. http://dx.doi.org/10.5038/1827-806X.43.1.4

Beres, M., Luetscher, M., Olivier, R. (2001). Integration of ground-penetrating radar and microgravimetric methods to map shallow caves, Journal of Applied Geophysics, 46(4), 249-262.

Bosse, M., Zlot, R., & Flick, P. (2012). Zebedee: Design of a spring-mounted 3-d range sensor with application to mobile mapping. IEEE Transactions on Robotics, 28(5), 1104-1119.

Buchroithner M.F. & Gaisecker T., 2009 - Terrestrial laser scanning for the visualization of a complex dome in an extreme alpine cave system. In: Photogrammetrie-Fernerkundung-Geoinformation (PFG), 4: 329-339.

Buchroithner M.F., Petters C., & Pradhan B., 2012 - Three-dimensional visualization of the world-class prehistoric site of the Niah Great Cave, Borneo, Malaysia. In: Kremers H. (Ed.), Proceedings of the Digital Cultural Heritage Interdisciplinary Conference. Saint-Dié-des-Vosges, France: 2 p.

Burens A., Grussenmeyer P., Carozza L., Leveque F., Guillemin S. & Mathe V., 2014 - Benefits of an accurate 3D documentation in understanding the status of the Bronze Age heritage cave "Les Fraux" (France). International Journal of Heritage in the Digital Era, 3 (1): 179-196. http://dx.doi.org/10.1260/2047-4970.3.1.179

Canevese E.P., Tedeschi R., Forti P. & Mora P., 2008 - The use of laser scanning techniques in extreme contexts: the case of Naica Caves (Chihuahua, Mexico). Geologia tecnica & ambientale (Journal of technical & environmental geology), 2: 19-37.

Canevese E.P., Forti P, Naseddu A., Ottelli L. & Tedeschi R., 2011 - Laser scanning technology for the hypogean survey: the case of Santa Barbara karst system (Sardinia, Italy). Acta Carsologica, 40 (1): 65-77.

Caprioli, M., Minchilli, M., Scognamiglio, A., & Strisciuglio, G. (2003). Using photogrammetry and laser scanning in surveying monumental heritage: le Grotte di Castellana. International Archives of Photogrammetry Remote Sensing and Spatial Information Sciences, 34(5/W12), 107-110.

Chamberlain, A.T., Sellers, W., Proctor, C., Coard, R. (2000). Cave Detection in Limestone using Ground Penetrating Radar, Journal of Archaeological Science, 27(10), 957-964,

Citton, P., Romano, M., Salvador, I., Avanzini, M. (2017). Reviewing the upper Pleistocene human footprints from the 'Sala dei Misteri'in the Grotta della Bàsura (Toirano, northern Italy) cave: An integrated morphometric and morpho-classificatory approach. Quaternary Science Reviews, 169, 50-64.

Cignoni, P., Ganovelli, F., Gobbetti, E., Marton, F., Ponchio, F. and Scopigno, R. (2005): Batched multi triangulation, in: IEEE Visualization, 2005, VIS 05, 23–28 October 2005, Minneapolis, Minnesota, USA, 207–214, doi:10.1109/VISUAL.2005.1532797.

Cosso, T., Ferrando, I., Orlando, A. (2014). Surveying and mapping a cave using 3d laser scanner: the open challenge with free and open source software. The International Archives of Photogrammetry, Remote Sensing and Spatial Information Sciences, 40(5), 181.

Doering, T., Collins, L., & Branas, C. (2006). Preacher's Cave high definition survey and 3D laser scanning project, Eleuthera, Bahamas. Scanning.

Donelan, J., 2002. Making prehistory, Computer Graphics World, March, pp. 32-33.

Droppa, A. (1964). Domica, plán 1:1000. Mapový archív SMOPaJ, ev. č. 16212.

Droppa, A. (1972). Príspevok k vývoju jaskyne Domica. Československý kras, 22, 65-72.

El-Hakim, S. F., Fryer, J., & Picard, M. (2004). Modelling and visualization of aboriginal rock art in the Baiame cave. International Archives of Photogrammetry and Remote Sensing, 35(5), 990-995.

Fabbri, S., Sauro, F., Santagata, T., Rossi, G., De Waele, J. (2017). High-resolution 3-D mapping using terrestrial laser scanning as a tool for geomorphological and speleogenetical studies in caves: An example from the Lessini mountains (North Italy). Geomorphology, 280, 16-29.

Fryer J.G., Chandler J.H. & El-Hakim S.F., 2005 - Recording and modelling an aboriginal cave painting: with or without laser scanning? International Archives of Photogrammetry, Remote Sensing and Spatial Information Sciences, 36 (5/W17): 1-8.

Gaál, Ľ. Gruber, P. (2014). Jaskynný systém Domica-Baradla. Jaskyňa, ktorá nás spája. Aggtelek (Aggteleki Nemzeti park), 512.

Gallay, M., Kaňuk, J., Hochmuth, Z., Meneely, J., Hofierka, J., Sedlák, V. (2015): Large-scale and high-resolution 3-D cave mapping by terrestrial laser scanning: a case study of the Domica Cave, Slovakia. International Journal of Speleology. 44(3), 277-291.

Gallay, M., Hochmuth, Z., Kaňuk, J., Hofierka, J. (2016). Geomorphometric analysis of cave ceiling channels mapped with 3D terrestrial laser scanning. Hydrology and Earth System Sciences, 20, 1827-1849.

Gašinec, J., Gašincová, S., Černota, P., Staňková, H. (2012). Zastosowanie naziemnego skaningu laserowego do monitorowania lodu gruntowego w Dobszyńskiej Jaskini Lodowej. Inżynieria Mineralna, 13, 31-42.

Gede, M., Petters, C., Nagy, G., Nagy, A., Mészáros, J., Kovács, B., & Egri, C. (2013). Laser scanning survey in the Pálvölgy Cave, Budapest. In Proceedings of the 26th International Cartographic Conference. International Cartographic Association, Dresden (p. 905).

Girardeau-Montaut, D. (2018). CloudCompare 2.10.2 Zephyrus. http://www.cloudcompare.org/.

Gómez-lende, M., Sánchez-Fernández, M. (2018). Cryomorphological Topo-graphies in the Study of Ice Caves. Geosciences, 8(8), 274.

González-Aguilera D.,Muñoz A.L., Lahoz J.G., Herrero J.S., Corchón M.S. & García E., 2009 - Recording and modeling Paleolithic caves through laser scanning. 2009 International Conference on Advanced Geographic Information Systems & Web Services: 19-26.

González-Aguilera, D., Muñoz-Nieto, A., Gómez-Lahoz, J., Herrero-Pascual, J., Gutierrez-Alonso, G. (2009). 3D digital surveying and modelling of cave geometry: Application to paleolithic rock art. Sensors, 9(2), 1108-1127.

Grussenmeyer, P., Landes, T., Alby, E., & Carozza, L. (2010). High resolution 3D recording and modelling of the Bronze Age cave "Les Fraux" in Périgord (France). Int. Arch. Photogramm. Remote Sens. Spat. Inf. Sci, 38, 262-267.

Hämmerle, M., Höfle, B., Fuchs, J., Schröder-Ritzrau, A., Vollweiler, N., & Frank, N. (2014). Comparison of kinect and terrestrial lidar capturing natural karst cave 3-d objects. IEEE Geoscience and Remote Sensing Letters, 11(11), 1896-1900.

Hofierka, J., Šašak, J., Šupinský, J., Gallay, M., Kaňuk, J., Sedlák, V. (2017). 3D mapovanie krajiny pomocou pozemného a leteckého laserového skenovania. Životné prostredie, 51, 21-27.

Hofierka, J., Gallay, M., Bandura, P., Šašak, J. (2018). Identification of karst sinkholes in a forested karst landscape using airborne laser scanning data and water flow analysis. Geomorphology, 308, 265-277.

Hochmuth, Z. (2014). Mapovanie prepojenia Čertovej diery a Domice. Spravodaj Slovenskej speleologickej spoločnosti. 45, 3, 18-23.

Kaul, L., Zlot, R., Bosse, M. (2016). Continuous-Time Three-Dimensional Mapping for Micro Aerial Vehicles with a Passively Actuated Rotating Laser Scanner. Journal of Field Robotics, 33(1), 103-132.

Kazhdan, M., Hoppe, H. (2013). Screened poisson surface reconstruction. ACM Transactions on Graphics (ToG), 32(3), 29.

Kordić, B., Đapo, A., & Pribičević, B. (2012, May). Application of terrestrial laser scanning in the preservation of fortified caves. In FIG Working Week 2012: Knowing to manage the territory, protect the environment, evaluate the cultural heritage.

Kregar, K., Vrabec, M., & Grigillo, D. (2019, January). Developing a robust workflow for acquisition of high-resolution full-3D cave topography, surface topography integration, and digital structural mapping. In Geophysical Research Abstracts (Vol. 21).

Kuda, F., Kajzar, V., Divíšek, J., Kukutsch, R. (2014). Aplikace pozemního laserového skenování v geovědních disciplínách. Praha (Ústav geoniky Akademie věd České republiky, v.v.i.).

Leonov, A. V., Anikushkin, M. N., Bobkov, A. E., Rys, I. V., Kozlikin, M. B., Shunkov, M. V., ... & Baturin, Y. M. (2014). Development of a virtual 3D model of Denisova Cave in the Altai Mountains. Archaeology, Ethnology and Anthropology of Eurasia, 42(3), 14-20.

Lerma, J. L., Navarro, S., Cabrelles, M., Villaverde, V. (2010). Terrestrial laser scanning and close range photogrammetry for 3D archaeological documentation: the Upper Palaeolithic Cave of Parpalló as a case study. Journal of Archaeological Science, 37(3), 499-507.

Lyons-Baral J., 2012 - Using terrestrial LiDAR to map and evaluate hazards of Coronado Cave, Coronado National Memorial, Cochise County, AZ. Arizona Geology Magazine, Summer: 1-4.

Marsico, A., Infante, M., Iurilli, V., Capolongo, D. (2015). Terrestrial laser scanning for 3D cave reconstruction: Support for geomorphological analyses and geoheritage enjoyment and use. In Hydrogeological and Environmental Investigations in Karst Systems. Springer, 543-550.

McFarlane D.A., Buchroithner M., Lundberg J., Petters C., Roberts W. & Van Rentergem G.,2013 - Integrated three-dimensional laser scanning and autonomous drone surface- photogrammetry at Gomantong caves, Sabah, Malaysia. In: Bosak P., & Filippi M. (Eds.), Proceedings of the 16th International Congress of Speleology, Brno, 2: 317-319.

Milius J. & Petters C., 2012 - Eisriesenwelt – from laser scanning to photo – realistic 3D model of the biggest ice cave on Earth. In: Jekel T., Car A., Strobl J. & Griesebner G. (Eds.), GI-Forum 2012: Geovisualization, Society and Learning. WichmannVerlag, Heidelberg: Salzburg, Austria: 513-523.

Murphy, P. J., Parr, A., Strange, K., Hunter, G., Allshorn, S., Halliwell, R. A., ... & Westerman, A. R. (2005). Investigating the nature and origins of Gaping Gill Main Chamber, North Yorkshire, UK, using ground penetrating radar and lidar. Cave and Karst Science, 32(1), 25.

Nash, G. H., & Beardlsey, A. (2013). The Survey of Cathole Cave, Gower Peninsula, South Wales. Proceedings of the University of Bristol Spelaeological Society, 26(1), 73-83.

Nocerino, E., Menna, F., Farella, E., Remondino, F. (2019). 3D virtualization of an underground semi-submerged cave system. International Archives of the Photogrammetry, Remote Sensing and Spatial Information Sciences, (2/W15), 857-864.

Novoveský, A. (1974). Domica, mapa 1:500. Mapový archív SMOPaJ, ev. č. 09724.

Novoveský, A. (1975). Technická správa, Domica 111-I-13. Geologický prieskum, n.p., Geologická služba podniku, geologická oblasť Rožňava. Slovenské múzeum ochrany prírody a jaskyniarstva.

Núñez, M. A., Buill, F., Edo, M. (2013). 3D model of the Can Sadurní cave. Journal of archaeological Science, 40(12), 4420-4428.

Perperidoy, D. G., Tzortzioti, E., & Sigizis, K. (2010). A new methodology for surveying and exploring complex environments using 3D scanning. In FIG Congress (pp. 1-14).

Petrović, A. S., Ćalić, J., Spalević, A., & Pantić, M. (2018). Relations between surface and underground karst forms inferred from terrestrial laser scanning. Geological Society, London, Special Publications, 466(1), 107-120.

Petters C., Milius J., Buchroithner M.F, 2011 - Eisriesenwelt: terrestrial laser scanning and 3D visualisation of the largest ice cave on Earth. In: Proceedings of the European LiDAR Mapping Forum. Salzburg, Austria: 10 p.

Peterson, T., Berg, J. (2001). Karst mapping with geophysics at Mystery Cave State Park, Minnesota. Minnesota Department of Natural Resources Ground Water and Climatology Section Report, 10.

Plan, L., Roncat, A., Marx, G. (2013). Detailed morphologic analysis of palaeotraun gallery using a terrestrial laser scan (Dachstein-Mammuthöhle, upper Austria). In Proceedings of the 16th International Congress of Speleology, 1, 399-401.

Potenziani, M., Callieri, M., Dellepiane, M., Corsini, M., Ponchio, F., Scopigno, R., (2015). 3DHOP: 3D Heritage Online Presenter. Computers & Graphics, 52, 129-141.

Potree (2021). Available online: http://www.potree.org/. (accessed on 20 August 2021).

Pucci, B., & Marambio Castillo, A. E. (2009). Olerdola's cave, Catalonia past and present: a virtual reality reconstruction from terrestrial laser scanner and gis data. In 3rd. International Workshop 3D Virtual Reconstruction and Visualization of Complex Architectures (pp. 1-14).

Pukanska, K., Bartoš, K., Bella, P., Sabová, J. (2017). Comparison of non-contact surveying technologies for modelling underground morphological structures. Acta Montanistica Slovaca, 22(3), 246-256.

Radicioni, F., Rossi, G., Tosi, G., & Marsili, R. (2019, May). Non contact shape and dimension measurements by LIDAR techniques of one of the biggest Italian caverns. In Journal of Physics: Conference Series (Vol. 1249, No. 1, p. 012019). IOP Publishing.

Rapidlasso GmbH. LAStools. Available online: https://rapidlasso.com/lastools/ (accessed on 1 August 2019).

Robson-Brown, K., Chalmers, A., Saigol, T., Green, C., D'errico, F. (2001). An automated laser scan survey of the Upper Palaeolithic rock shelter of Cap Blanc. Journal of Archaeological Science, 28(3), 283-289.

Roncat A., Dublyansky Y., Spötl C, Dorninger P. & Pfeifer N., 2011 - A full-3D laser-scan mapping of a hypogene cave: a morphogenetic study of Märchenhöhle, Austria. Geophysical Research Abstracts. EGU 2011, Vienna, 13, 14039.

Rüther, H., Chazan, M., Schroeder, R., Neeser, R., Held, C., Walker, S. J., ... & Horwitz, L. K. (2009). Laser scanning for conservation and research of African cultural heritage sites: the case study of Wonderwerk Cave, South Africa. Journal of Archaeological Science, 36(9), 1847-1856.

Santagata, T., Lugli, S., Camorani, M. E., Ercolani, M. (2015). Laser scanner survey and tru view applications of the" Grotta della lucerna"(Ravenna, Italy), a roman mine for lapis specularis. In Hypogea 2015: proceedings of international congress of speleology in artificial cavities: Italy, Rome, march 11/17, 2015, 1, 411-416.

Santos Delgado G., Martínez Rubio J., Silva Barroso P.G., Sánchez Moral S., Cañaveras Jiménez J.C. & De la Rasilla Vives M., 2012 - Contribución al conocimiento de la cueva de El Sidrón (Piloña, Asturias) con técnicas de láser escáner 3D. In: González A. et al. (Eds.), Avances de la Geomorfología en España 2010-2012. Actas de la XII Reunión Nacional de Geomorfología, Santander, 17-20 September 2012: 255-258.

Schütz, M., Ohrhallinger, S., Wimmer, M. 2020. Fast Out-of-Core Octree Generation for Massive Point Clouds. Computer Graphics Forum, 39(7), 1-13.

Schütz, M. Potree: Rendering Large Point Clouds in Web Browsers. Engineer Diploma Thesis, Vienna University of Technology, Vienna, Austria, 2016; p. 92.

Scheiblauer, C. Interactions with Gigantic Point Clouds. Ph.D. Thesis, Vienna University of Technology, Vienna, Austria, 2014; p. 203.

Silvestre I., Rodrigues J.I., Figueiredo M. & Veiga-Pires C., 2015 - High-resolution digital 3D models of Algar do Penico Chamber: limitations, challenges, and potential. International Journal of Speleology, 44 (1): 25-35. http://dx.doi.org/10.5038/1827-806X.44.1.3

Scopigno, R.; Callieri, M.; Delleppiane, M.; Ponchio, F.; Potenziani, M. Delivering and using 3D models on the web: Are we ready? Virtual Archaeol. Rev. 2017, 8, 1–9.

Stipanov, M., Bakarić, V., Eškinja, Z. (2008). ROV use for cave mapping and modeling. IFAC Proceedings Volumes, 41(1), 208-211.

Šupinský, J., Kaňuk, J., Hochmuth, Z., Gallay, M. (2019). Detecting dynamics of cave floor ice with selective cloud-to-cloud approach. The Cryosphere, 13, 11, 2835-2851.

Thibault G., 2001 - 3D modeling of the Cosquer cave by laser survey. International Newsletter on Rock Art, No. 28: 25–29

Triantafyllou, A., Watlet, A., Le Mouélic, S., Camelbeeck, T., Civet, F., Kaufmann, O., ... Vandycke, S. (2019). 3-D digital outcrop model for analysis of brittle deformation and lithological mapping (Lorette cave, Belgium). Jour. of Struc. Geol., 120, 55-66.

Tsakiri, M., Sigizis, K., Billiris, H., & Dogouris, S. (2007, September). 3D laser scanning for the documentation of cave environments. In 11th ACUUS Conference: Underground Space: Expanding the Frontiers.

Tyszkowski, S., Kramkowski, M., Wisniewska, D., & Urban, J. (2016, April). Use of terrestrial laser scanning for the documentation of quaternary caves. In EGU General Assembly Conference Abstracts (Vol. 18).

Ullrich, A., Schwarz, R., & Kager, H. (2003). Using hybrid multi-station adjustment for an integrated camera laser-scanner system. na.

Wenger, R. (2004). La balise de positionnement U-GPS (Underground-GPS). ISSKA Rapport Annuel (Swiss Institute for Speleology and Karst Studies, La Chaux-de-Fonds 2004), 13-14.

Westerman, A. R., Pringle, J. K., & Hunter, G. (2003). Preliminary LIDAR survey results from Peak Cavern Vestibule, Derbyshire, UK. Cave and Karst Science, 30(3), 129-130.

Yakar, M., Ulvi, A., & Toprak, A. S. (2016). The Use of Laser Scanner in Caves, Encountered Problems and Solution Suggestion. Universal Journal of Geoscience, 4(4), 81-88.

Zeid, N. A., Bignardi, S., Russo, P., & Peresani, M. (2019). Deep in a Paleolithic archive: Integrated geophysical investigations and laser-scanner reconstruction at Fumane Cave, Italy. Journal of Archaeological Science: Reports, 27, 101976.

Zlot, R., Bosse, M. (2014). Three-dimensional mobile mapping of caves. Journal of Cave & Karst Studies, 76(3).